Original paper

Navrotskyite, $K_2Na_{10}(UO_2)_3(SO_4)_9 \cdot 2H_2O$, a new sodium and potassium uranyl-sulfate mineral from the Blue Lizard mine, Red Canyon, White Canyon District, San Juan County, Utah

Travis A. OLDS[1]*, Anthony R. KAMPF[2], Samuel N. PERRY[3], Xiaofeng GUO[4], Joe MARTY[5], Timothy P. ROSE[6], Peter C. BURNS[3,7]

[1] *Section of Minerals and Earth Sciences, Carnegie Museum of Natural History, 4400 Forbes Avenue, Pittsburgh, Pennsylvania 15213, USA; oldst@carnegiemnh.org*
[2] *Mineral Sciences Department, Natural History Museum of Los Angeles County, 900 Exposition Boulevard, Los Angeles, CA 90007, USA*
[3] *Department of Civil and Environmental Engineering and Earth Sciences, University of Notre Dame, Notre Dame, IN 46556, USA*
[4] *Department of Chemistry, Washington State University, Pullman, WA 99163, USA*
[5] *5199 East Silver Oak Road, Salt Lake City, UT 84108, USA*
[6] *Nuclear and Chemical Sciences Division, Lawrence Livermore National Laboratory, Livermore, CA 94550, USA*
[7] *Department of Chemistry, University of Notre Dame, Notre Dame, IN 46556, USA*
** Corresponding author*

Navrotskyite (IMA 2019-026), $K_2Na_{10}(UO_2)_3(SO_4)_9 \cdot 2H_2O$, is a new potassium-sodium-uranyl-sulfate mineral from the Blue Lizard mine, San Juan County, Utah, USA. The new mineral occurs on sandstone and asphaltite matrix in close association with belakovskiite, blödite, bobcookite, changoite, fermiite, ferrinatrite, ilsemannite, ivsite, meisserite, pseudomeisserite-(NH_4), seaborgite and tamarugite. Navrotskyite is orthorhombic, space group *Pbcm* (#57), with unit cell parameters $a = 5.4456(13)$, $b = 21.328(5)$, $c = 33.439(8)$ Å, $V = 3883.8(2)$ Å^3 and $Z = 4$. Crystals are acicular tapered needles up to about 1 mm in length, typically occurring as radial sprays and tightly intergrown aggregates resembling fibre-optic bundles. Crystals are elongated on [100] and exhibit only the {012} prism form, resulting in diamond-shaped cross-sections. The terminations are generally not well-formed, but broken crystals are truncated by good {100} cleavage. No twinning was observed. Navrotskyite is pale greenish yellow in color, has a white or very pale-yellow streak and fluoresces neon yellow green under both long- and short-wave UV. It is transparent with vitreous to silky luster. The mineral exhibits a splintery, uneven fracture and has a Mohs hardness of about 2. The calculated density based on the empirical formula is 3.46 g/cm^3. The mineral is optically biaxial (–), with $\alpha = 1.520(2)$, $\beta = 1.557(2)$ and $\gamma = 1.565(2)$ (white light). The measured $2V$ is 48.2(5)° and the calculated $2V$ is 48.9°. Dispersion is imperceptible and no pleochroism was observed. The optical orientation is X = **a**, Y = **c**, Z = **b**. The empirical formula is $K_{2.06}Na_{9.98}U_{3.02}S_{8.98}O_{44}H_{3.97}$ based on 44 O *apfu*. The eight strongest powder X-ray diffraction lines are [d_{obs} Å(I)(hkl)]: 5.28(100)(110), 3.050(44)(049, 119), 10.70(43)(020), 3.845(36)(046,134,116), 3.225(30)(153), 3.533(29)(060,061,136), 2.822(29)(139) and 5.59(27)(006). The crystal structure of navrotskyite ($R_1 = 0.0289$ for 4032 reflections with $I > 2\sigma I$) contains infinite $[(UO_2)(SO_4)_3]^{4-}$ chains that extend along [100] and that link to neighbouring chains *via* a complex network of K–O and Na–O bonds. Related topologies based on the same UL_3-type chain are also observed in the minerals fermiite, meisserite and pseudomeisserite-(NH_4), all of which occur in the same general assemblage as navrotskyite.

Keywords: Navrotskyite, uranyl sulfate, uranium, crystal structure, chains, Raman
Received: 13 March 2022; accepted: 19 June 2023; handling editor: F. Laufek

1. Introduction

Sixty-two uranyl-sulfate minerals have been described to date, recently overtaking the 53 known uranyl phosphates, making sulfates the most numerous subgroup of uranyl minerals containing polyoxoanions. While uranyl phosphates almost exclusively form structures based on sheet topologies, uranyl-sulfate structures, in addition to sheets of polyhedra (i.e. the zippeite group), tend to contain isolated clusters and infinite chains of polyhedra (~40%) (Gurzhiy and Plášil 2019). This is especially true of the uranyl sulfates found in the mines in Red Canyon; most species occurring there contain structural units with cluster or chain topologies and this tendency is likely related to how the minerals formed. The semi-arid climate in Red Canyon includes periodic torrential rains. Large mines, such as the Blue Lizard, have relatively consistent temperature throughout; however, the unique microclimate formed during oscillations of wet and dry periods cause flooding and slow-to-develop, but large fluctuations in relative humidity underground. The uranyl-sulfate minerals have formed as efflorescent coat-

Fig. 1 – Intergrown short prisms of navrotskyite with white ivsite. The field of view is 0.84 mm across.

Tab. 1 Chemical composition of navrotskyite.

Constituent	Theoretical	Mean	Range	Stand. Dev.	Standard
Na_2O	15.35	15.37	14.06–16.39	0.87	albite
K_2O	4.67	4.82	4.12–5.50	0.55	orthoclase
UO_3	42.51	42.94	39.59–45.09	2.16	U metal
SO_3	35.69	35.74	34.84–37.19	0.96	anhydrite
H_2O*	1.78	1.78	–	–	–
Total	100.00	100.66			

* based on the structure

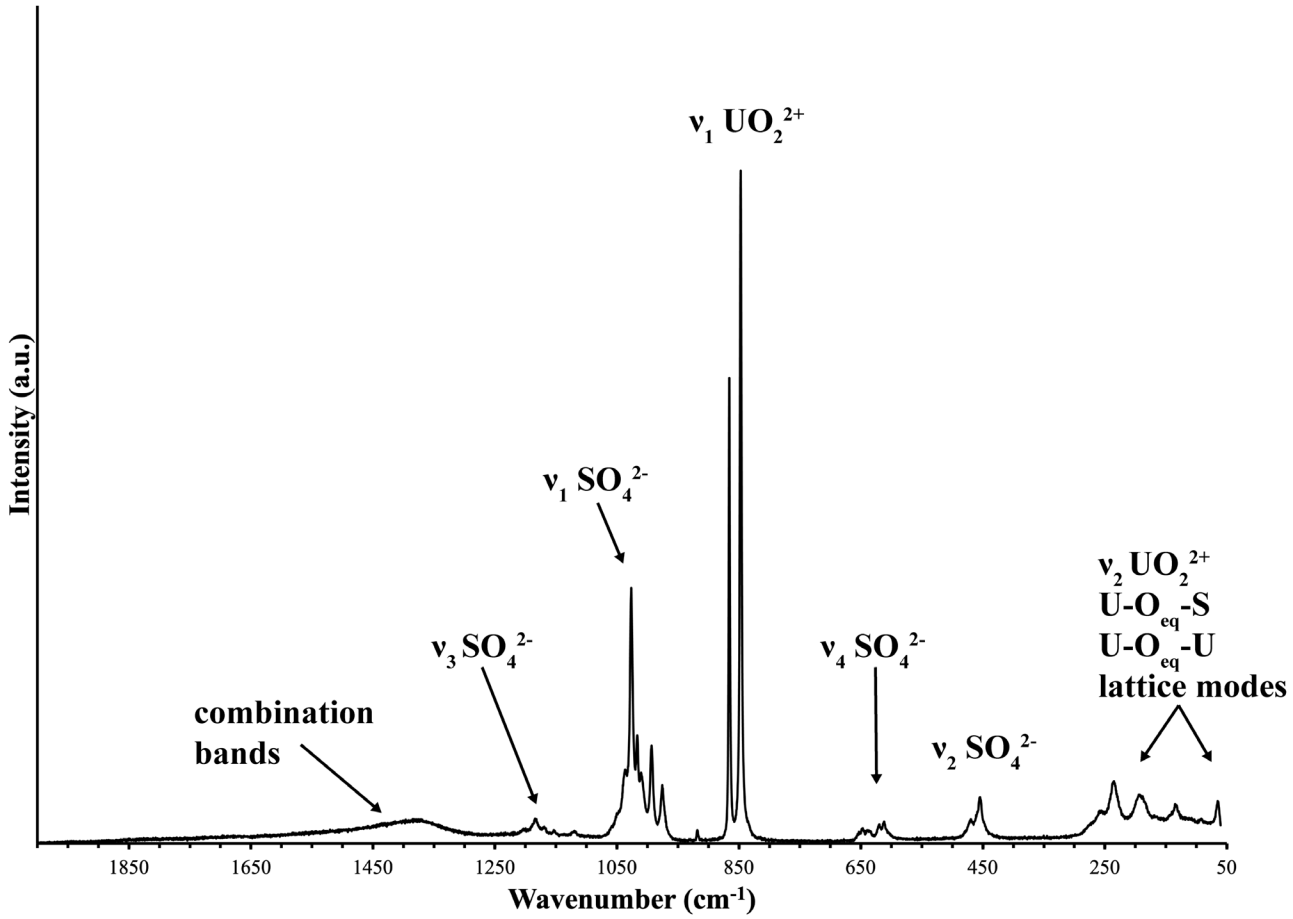

Fig. 2 The Raman spectrum of navrotskyite taken with a 785 nm laser from 2000–60 cm^{-1}.

ings from groundwater seepage, and often these crusts contain dozens of species in a small area. Blooms of mineralization between wet and dry periods have likely contributed to the observed diversity of minerals.

Navrotskyite is named for American physical chemist, geochemist and materials scientist Dr. Alexandra Navrotsky (b. 1943). Her research interests have centred about relating microscopic features of structure and bonding to macroscopic thermodynamic behaviour in minerals, ceramics and other complex materials. She has published over 700 scientific papers and has received numerous awards. In 2002, she was awarded the Benjamin Franklin Medal in Earth Science. In 2004, she was elected a Fellow of The Mineralogical Society (Great Britain) and awarded the Urey Medal (the highest career

Tab. 2 Powder X-ray data (d in Å) for navrotskyite. Only $I \geq 3$ calculated lines are listed.

I_{obs}	d_{obs}	d_{calc}	I_{calc}	h k l
43	**10.70**	10.6704	48	0 2 0
25	7.74	7.7163	28	0 2 3
27	**5.59**	5.5860	33	0 0 6
100	**5.28**	5.2775	100	1 1 0
12	4.90	4.9489	11	0 2 6
26	4.78	4.8144	19	0 4 3
		4.7718	14	1 1 3
		4.6599	4	1 2 2
10	4.311	4.3246	10	1 3 0
26	4.039	4.0330	27	1 3 3
		3.8582	9	0 4 6
36	**3.845**	3.8429	3	1 3 4
		3.8362	32	1 1 6
		3.5568	10	0 6 0
29	**3.533**	3.5369	4	0 6 1
		3.5160	22	0 2 9
		3.4196	3	1 3 6
27	3.385	3.3892	25	0 6 3
		3.3595	4	1 5 0
		3.3132	3	1 4 5
30	**3.225**	3.2172	33	1 5 3
		3.1182	4	1 5 4
44	**3.050**	3.0537	31	0 4 9
		3.0427	20	1 1 9
6	3.002	3.0090	5	1 3 8
		3.0002	3	0 6 6
		2.9819	4	1 4 7
8	2.874	2.8790	8	1 5 6
		2.8552	3	0 6 7
29	**2.822**	2.8219	30	1 3 9
		2.7930	8	0 0 12
12	2.715	2.7233	7	2 0 0
		2.7020	4	0 2 12
		2.6927	3	2 1 1
23	2.657	2.6676	6	0 8 0
		2.6603	12	1 7 0
		2.6520	6	1 7 1
		2.6387	4	2 2 0
8	2.582	2.5879	4	1 7 3
		2.5721	3	0 6 9
		2.5681	5	2 2 3
22	2.483	2.4945	17	1 5 9
		2.4686	9	1 1 12
		2.4479	6	2 0 6
21	2.384	2.4018	6	1 7 6
		2.3859	6	2 2 6
		2.3704	9	2 4 3
		2.1870	3	0 2 15
8	2.172	2.1741	3	1 9 0
		2.1647	3	1 7 9
8	2.130	2.1229	7	2 6 3
5	2.0619	2.0680	4	1 9 5
		2.0609	3	0 4 15
19	2.0269	2.0325	12	2 4 9
		2.0261	8	1 9 6
		2.0165	4	2 6 6
		2.0071	3	0 8 11
12	1.9869	1.9935	5	0 10 6
		1.9851	7	1 3 15
9	1.9454	1.9498	9	2 0 12
		1.9291	3	0 8 12
9	1.9189	1.9263	6	1 7 12
		1.9181	4	2 2 12
5	1.8935	1.9057	3	2 8 0
		1.9026	3	2 8 1
		1.8920	3	0 6 15
18	1.8612	1.8699	5	2 6 9
		1.8620	5	0 0 18
		1.8605	8	1 5 15
		1.8514	3	1 7 13
		1.8343	3	0 2 18
9	1.8079	1.8036	5	2 8 6
10	1.7706	1.7856	3	1 11 4
		1.7559	11	1 1 18
16	1.7443	1.7396	3	0 12 4
		1.7377	7	3 3 3
		1.7370	3	1 11 6
15	1.7156	1.7210	6	3 1 6
		1.7156	3	1 9 12
4	1.6776	1.6779	3	3 3 6
10	1.6509	1.6523	5	3 5 3
		1.6434	4	2 4 15
6	1.6077	1.6086	4	2 10 6
4	1.5820	1.5906	4	3 3 9
7	1.5577	1.5538	3	2 6 15
5	1.5414	1.5448	4	1 13 4
		1.5371	3	2 0 18
14	1.5248	1.5293	4	1 11 12
		1.5243	3	3 5 9
		1.5183	4	3 1 12
7	1.4951	1.4973	3	1 3 21

honour of the European Association of Geochemistry). In 2006, she received the Harry H. Hess Medal of the American Geophysical Union. In October 2009, she received the Roebling Medal, the highest honour awarded by the Mineralogical Society of America.

The description is based on three cotype specimens (all micromounts) deposited in the collections of the Natural History Museum of Los Angeles County, 900 Exposition Boulevard, Los Angeles, CA 90007, USA, catalogue numbers 73574, 73575 and 73576. The IMA-CNMNC approved mineral abbreviation for navrotskyite is Nvr (Warr 2021).

2. Occurrence

Navrotskyite occurs underground in the Blue Lizard mine, Red Canyon, White Canyon District, San Juan County, Utah. The Blue Lizard mine (37°33'26"N 110°17'44"W) is situated on the northern ridge of Red Canyon, roughly 1 km to the northeast of the Markey mine and ~22 km southeast of Good Hope Bay on Lake Powell. Detailed historical and geologic information on the Blue Lizard mine is provided elsewhere (Kampf et al. 2015), and is primarily derived from a report by Chenoweth (1993). Access to the underground workings is no longer possible, as the entrance was gated in 2021.

Abundant secondary uranium mineralization in Red Canyon is associated with post-mining oxidation of asphaltite-rich sandstone beds laced with uraninite, coffinite and sulfides in the damp underground environment. Navrotskyite was found in an area rich in K-bearing sulfates (metavoltine, voltaite, zincovoltaite), and was noted as a close associate with seaborgite, $LiK_2Na_6(UO_2)(SO_4)_5(SO_3OH)(H_2O)$ (Kampf et al. 2021) in several specimens. Potassium enrichment has so far not been observed in secondary uranyl mineralization elsewhere in the Blue Lizard mine, nor in any of the nearby U deposits in Red Canyon that we have investigated. It is likely that K and Li are sourced from Li- and K-bearing clays in the sediments. Other associated minerals include belakovskiite, blödite, bobcookite, changoite, fermiite, ferrinatrite, ilsemannite, ivsite, meisserite, pseudomeisserite-(NH_4) and tamarugite.

3. Physical and optical properties

Crystals are acicular or thin tapered needles up to about 1 mm in length, typically occurring in radial sprays or as tightly intergrown aggregates resembling fibre-optic bundles (Fig. 1). The terminations are generally not well-formed, but broken crystals are truncated by good {100} cleavage. Crystals exhibit the prism form {012}, resulting in diamond-shaped cross-sections. No other forms were observed, nor was twinning observed. Navrotskyite is pale greenish yellow, has a white or very pale-yellow streak and fluoresces neon yellow green under both long- and short-wave ultraviolet illumination. Aggregates sometimes appear greenish blue due to underlying ferrinatrite and coatings of an amorphous hydrated Mo-oxide presumed to correspond to ilsemannite. It is transparent with vitreous to silky luster and the mineral exhibits a brittle tenacity; long, thin crystals are flexible with splintery, uneven fracture and a Mohs hardness of about 2 based on scratch tests.

The density could not be measured because the mineral is soluble in H_2O (and Clerici solution). The calculated density based on the empirical formula and density calculated using the cell derived from PXRD data is 3.46 g/cm^3 and 3.45 g/cm^3 using the cell volume derived from the single-crystal X-ray diffraction study. The mineral is optically biaxial (–), with α = 1.520(2), β = 1.557(2) and γ = 1.565(2) (determined in

Tab. 3 Data collection and structure refinement details for navrotskyite.

Temperature	293(2) K
Structural Formula	$K_2Na_{10}(UO_2)_3(SO_4)_9 \cdot 2H_2O$
Space group	*Pbcm*
Unit cell dimensions	a = 5.4456(13) Å
	b = 21.328(5) Å
	c = 33.439(8) Å
V	3883.8(16) Å^3
Z	2
Density (for above formula)	3.453 g cm^{-3}
Absorption coefficient	13.428 mm^{-1}
F(000)	3696
Crystal size	4 × 4 × 5 µm
θ range	2.64 to 25.24°
Index ranges	$-6 \le h \le 6$, $-26 \le k \le 26$, $-41 \le l \le 41$
Reflections collected/unique	44551/4032; R_{int} = 0.09
Reflections with $I > 2\sigma I$	3837
Completeness to θ = 25.24°	99.9%
Refinement method	Full-matrix least-squares on F^2
Parameter/restraints	332/3
GoF	1.038
Final R indices [$I > 4\sigma I$]	R_1 = 0.0289, wR_2 = 0.0452
R indices (all data)	R_1 = 0.0509, wR_2 = 0.0498
Largest diff. peak/hole	+1.22/–1.24 e A^{-3}

$R_{int} = \Sigma|F_o^2 - F_o^2(\text{mean})|/\Sigma[F_o^2]$. GoF = $S = \{\Sigma[w(F_o^2 - F_c^2)^2]/(n-p)\}^{1/2}$. $R_1 = \Sigma||F_o| - |F_c||/\Sigma|F_o|$. $wR_2 = \{\Sigma[w(F_o^2 - F_c^2)^2]/\Sigma[w(F_o^2)^2]\}^{1/2}$; $w = 1/[\sigma^2(F_o^2) + (aP)^2 + bP]$ where a is 0.0114, b is 14.2186 and P is $[2F_c^2 + \text{Max}(F_o^2, 0)]/3$.

white light). The measured $2V$ is 48.2(5)° and the calculated $2V$ is 48.9°. Dispersion is imperceptible and no pleochroism was observed. The optical orientation is X = **a**, **Y** = **c**, Z = **b**. The Gladstone-Dale relationship was calculated; $1 - (K_p/K_C) = -0.003$ (superior) based on the empirical formula and –0.005 (superior) based on the ideal formula, in both cases using $k(UO_3) = 0.118$ (Mandarino 1976).

4. Chemical composition

Chemical analyses (6 points on 2 crystals) were performed on a JEOL JXA-8230 electron microprobe using Probe for EPMA software (Tab. 1). The analytical conditions used were 15 keV accelerating voltage, 3 nA beam current and a beam diameter of 10 μm. Raw X-ray intensities were corrected for matrix effects with the φρ(z) algorithm (Pouchou and Pichoir, 1985). Time-dependent intensity corrections were applied to Na, K and S. Because insufficient material was available for a direct determination of H_2O, it has been calculated based upon the structure determination (U+S = 12 *apfu*, O = 44 *apfu*). The empirical formula, calculated on the basis of 44 O *apfu*, is $K_{2.06}Na_{9.98}U_{3.02}S_{8.98}O_{44}H_{3.97}$. The ideal formula is $K_2Na_{10}(UO_2)_3(SO_4)_9 \cdot 2H_2O$, which requires Na_2O 15.35, K_2O 4.67, UO_3 42.51, SO_3 35.69, H_2O 1.78, total 100 wt. %.

Tab. 4 Atom coordinates and displacement parameters (Å²) for navrotskyite.

Site	*x*/*a*	*y*/*b*	*z*/*c*	U_{eq}
U1	0.23183(6)	0.82129(2)	0.25	0.00886(8)
U2	0.26713(4)	0.70323(2)	0.41392(2)	0.00941(6)
S1	0.6950(3)	0.34189(7)	0.48078(4)	0.0100(3)
S2	0.1233(3)	0.67776(7)	0.30985(5)	0.0092(3)
S3	0.3025(3)	0.85138(7)	0.36007(5)	0.0123(3)
S4	0.3461(4)	0.98870(11)	0.25	0.0127(5)
S5	0.1488(3)	0.53797(7)	0.40134(5)	0.0103(3)
K1	0.8076(3)	0.93900(8)	0.31790(5)	0.0309(4)
Na1	0.2327(7)	0.25	0.5	0.0235(8)
Na2	0.6757(7)	0.68312(17)	0.25	0.0214(9)
Na3	0.6496(5)	0.47365(12)	0.41573(8)	0.0215(6)
Na4	0.7976(7)	0.07201(16)	0.25	0.0204(9)
Na5	0.6566(5)	0.59104(12)	0.33911(8)	0.0195(6)
Na6	0.7813(5)	0.86602(16)	0.42471(9)	0.0393(8)
Na7*	0.032(2)	0.5144(5)	0.5001(5)	0.037(3)
O1	0.9616(8)	0.3351(2)	0.48109(14)	0.0189(11)
O2	0.6215(9)	0.4060(2)	0.47093(14)	0.0218(11)
O3	0.5747(8)	0.2982(2)	0.45186(13)	0.0172(10)
O4	0.5913(8)	0.3257(2)	0.52071(12)	0.0135(10)
O5	0.3739(8)	0.6590(2)	0.30037(13)	0.0162(11)
O6	0.0695(8)	0.7404(2)	0.29238(13)	0.0163(10)
O7	0.0810(8)	0.6802(2)	0.35327(13)	0.0158(10)
O8	0.9465(8)	0.6323(2)	0.29354(13)	0.0165(10)
O9	0.0765(10)	0.8708(3)	0.37849(19)	0.0428(16)
O10	0.5032(8)	0.8909(2)	0.37413(15)	0.0216(12)
O11	0.3595(9)	0.7852(2)	0.36980(13)	0.0226(12)
O12	0.2836(11)	0.8572(2)	0.31651(13)	0.0366(14)
O13	0.0789(12)	0.9917(3)	0.25	0.0266(19)
O14	0.4539(9)	0.0181(2)	0.28551(14)	0.0239(12)
O15	0.4251(10)	0.9214(3)	0.25	0.0128(14)
O16	0.3721(8)	0.5372(2)	0.37753(14)	0.0177(11)
O17	0.9336(8)	0.5286(2)	0.37615(14)	0.0206(11)
O18	0.1591(8)	0.4886(2)	0.43214(13)	0.0170(10)
O19	0.1245(8)	0.5996(2)	0.42260(13)	0.0158(10)
O20	0.5187(12)	0.7837(3)	0.25	0.0250(17)
O21	0.9436(11)	0.8587(3)	0.25	0.0158(15)
O22	0.5496(8)	0.6723(2)	0.39708(13)	0.0167(10)
O23	0.9808(8)	0.7310(2)	0.43161(13)	0.0169(10)
OW1	0.7020(10)	0.5527(2)	0.46665(16)	0.0252(11)
H1A	0.586(9)	0.565(3)	0.4809(18)	0.02(2)
H1B	0.775(11)	0.583(2)	0.4572(19)	0.02(2)

5. Raman Spectroscopy

Raman spectroscopy was conducted on a Horiba XploRA PLUS. The spectrum recorded from 2000 to 60 cm^{-1} using a 785 nm laser is given in Fig. 2. A broad band with low intensity centred near 1370 cm^{-1} is attributed to combination bands. The split $\nu_3 (SO_4)^{2-}$ antisymmetric stretching vibrations occur as weak bands at 1196, 1184, 1169, 1153 and 1119 cm^{-1}. A complex set of medium and strong intensity bands at 1036 (1050 sh), 1026, 1016, 1010, 993 and 975 cm^{-1} are assigned to the $\nu_1(SO_4)^{2-}$ symmetric stretching vibrations. The weak band at 917 cm^{-1} is related to the $\nu_3 (UO_2)^{2+}$ antisymmetric stretching vibration, which is normally absent; however slight distortions lead to its activity here. The $\nu_1 (UO_2)^{2+}$ symmetric stretching vibration is present as two very intense bands at 866 and 847 cm^{-1}, corresponding to the two symmetrically independent U sites in navrotskyite. Using the empirical relationship developed by Bartlett and Cooney (1989), we have calculated the approximate uranyl oxygen ($U–O_{yl}$) bond lengths from the positions

Tab. 5 Anisotropic displacement parameters (Å^2) for navrotskyite.

	U^{11}	U^{22}	U^{33}	U^{23}	U^{13}	U^{12}
U1	0.01081(17)	0.00731(14)	0.00845(15)	0	0	–0.00041(15)
U2	0.01236(12)	0.00897(11)	0.00691(10)	–0.00011(9)	–0.00071(11)	–0.00093(11)
S1	0.0139(8)	0.0099(7)	0.0064(7)	0.0002(6)	–0.0004(6)	0.0017(6)
S2	0.0113(7)	0.0111(8)	0.0053(8)	0.0002(7)	–0.0005(6)	–0.0017(6)
S3	0.0177(9)	0.0114(7)	0.0080(7)	0.0009(6)	–0.0024(7)	–0.0047(6)
S4	0.0140(12)	0.0089(12)	0.0151(13)	0	0	–0.0014(9)
S5	0.0113(8)	0.0098(8)	0.0099(8)	0.0003(6)	–0.0001(6)	–0.0007(6)
K1	0.0324(10)	0.0364(9)	0.0239(9)	0.0047(7)	0.0022(7)	0.0080(8)
Na1	0.018(2)	0.0224(18)	0.030(2)	0.0050(16)	0	0
Na2	0.018(2)	0.027(2)	0.019(2)	0	0	0.0066(16)
Na3	0.0280(15)	0.0171(14)	0.0194(15)	0.0031(12)	–0.0022(13)	–0.0027(11)
Na4	0.020(2)	0.0124(18)	0.029(2)	0	0	0.0007(16)
Na5	0.0151(14)	0.0229(15)	0.0204(15)	0.0075(12)	0.0021(11)	0.0020(11)
Na6	0.0183(16)	0.071(2)	0.0286(17)	0.0237(15)	0.0001(14)	–0.0012(16)
Na7	0.023(6)	0.067(10)	0.020(3)	–0.004(7)	–0.009(4)	0.009(5)
O1	0.011(2)	0.025(3)	0.021(3)	–0.002(2)	0.000(2)	–0.001(2)
O2	0.037(3)	0.010(2)	0.019(3)	0.000(2)	0.008(2)	0.008(2)
O3	0.017(2)	0.022(2)	0.013(2)	–0.001(2)	–0.0049(19)	0.003(2)
O4	0.019(2)	0.015(2)	0.006(2)	0.0041(19)	–0.0017(18)	–0.0005(19)
O5	0.012(2)	0.024(3)	0.013(3)	0.005(2)	0.0029(19)	0.003(2)
O6	0.019(2)	0.015(3)	0.015(2)	0.007(2)	0.001(2)	0.0018(19)
O7	0.023(3)	0.019(2)	0.006(2)	0.001(2)	–0.0020(19)	–0.004(2)
O8	0.017(2)	0.020(3)	0.013(3)	0.000(2)	–0.002(2)	–0.008(2)
O9	0.022(3)	0.055(4)	0.052(4)	0.017(3)	0.014(3)	0.012(3)
O10	0.022(3)	0.016(3)	0.027(3)	–0.003(2)	–0.007(2)	–0.009(2)
O11	0.048(3)	0.009(3)	0.011(3)	0.0011(19)	–0.001(2)	–0.004(2)
O12	0.081(4)	0.018(2)	0.010(2)	0.0030(19)	–0.017(3)	–0.014(3)
O13	0.015(4)	0.014(4)	0.051(5)	0	0	0.004(3)
O14	0.028(3)	0.020(3)	0.023(3)	–0.011(2)	–0.002(2)	–0.001(2)
O15	0.010(3)	0.010(3)	0.018(4)	0	0	0.001(3)
O16	0.014(2)	0.019(3)	0.020(3)	0.003(2)	0.006(2)	0.0032(19)
O17	0.018(3)	0.018(3)	0.026(3)	–0.003(2)	–0.005(2)	–0.002(2)
O18	0.028(3)	0.011(2)	0.011(2)	0.0053(19)	0.001(2)	0.0020(19)
O19	0.022(3)	0.012(2)	0.014(3)	–0.0013(19)	0.0064(19)	–0.0036(19)
O20	0.019(4)	0.013(4)	0.043(5)	0	0	–0.003(3)
O21	0.010(3)	0.013(3)	0.025(4)	0	0	0.001(3)
O22	0.013(2)	0.020(3)	0.018(3)	0.001(2)	0.0029(19)	0.002(2)
O23	0.014(2)	0.021(3)	0.016(2)	–0.004(2)	–0.001(2)	0.000(2)
OW1	0.025(3)	0.022(3)	0.029(3)	–0.003(2)	0.008(3)	0.003(2)

of the $\nu_1(UO_2)^{2+}$ bands, which give 1.76 and 1.75 Å. The calculated values are in good agreement with average U–O_{yl} bond lengths from the X-ray data: U1, 1.759(4) Å, and U2, 1.768(4) Å.

Several weak overlapping bands between 651 and 610 cm^{-1} are attributed to the split, triply degenerate ν_4 (δ) $(SO_4)^{2-}$ bending vibrations, and those at 470 and 455 cm^{-1} to the split doubly degenerate ν_2 (δ) $(SO_4)^{2-}$ bending vibrations. We base the remaining assignments for the low wavenumber region on those provided by Plášil et al. (2010). The bands at 269 and 253 cm^{-1} are assigned to split ν_2 (δ) $(UO_2)^{2+}$ modes and one at 232 cm^{-1} to U–O_{eq}–S modes. The weak bands at 190 and 131 cm^{-1} are attributable to U–O_{eq}–U bending modes, and the remaining very weak bands at 87 and 64 cm^{-1} are unassigned lattice modes corresponding to U atom displacements. No modes belonging to K–O or Na–O stretching (~300 cm^{-1}) were observed.

6. X-ray crystallography and structure determination

6.1. Powder diffraction

X-ray powder diffraction data were recorded using a Rigaku R-Axis Rapid II curved imaging plate microdiffractometer with monochromatized Mo*K*α radia-

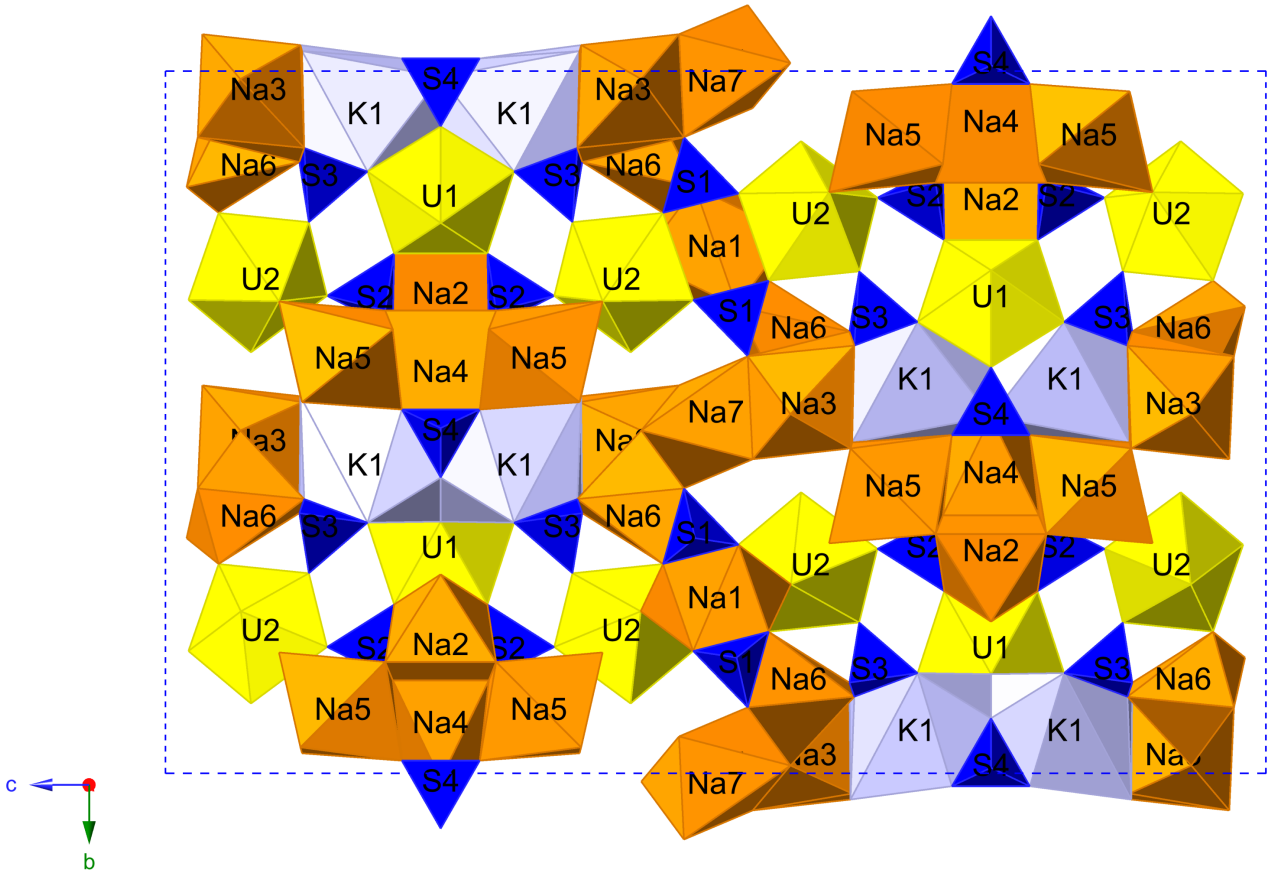

Fig. 3 The crystal structure of navrotskyite viewed down **a**. The unit cell is indicated by dashed blue lines.

tion. A Gandolfi-like motion on the ϕ and ω axes was used to randomize the sample. Observed *d* values and intensities were derived by profile fitting using JADE 2010 software (Materials Data, Inc.). Data are given in Tab. 2. Unit cell parameters refined from the powder data using JADE 2010 with whole pattern fitting are a = 5.4466(8) Å, b = 21.341(3) Å, c = 33.516(5) Å and V = 3895.8(10) Å^3.

6.2. Single-crystal X-ray diffraction and structure solution

A thin navrotskyite prism was chosen for the single-crystal X-ray diffraction study. Data were collected using Mo*K*α X-rays and an Apex II CCD-based detector mounted to a Bruker Apex II three-circle diffractometer. The Apex 3 software package was used for processing collected diffraction data, including corrections for background, polarization and Lorentz effects. A multi-scan semi-empirical absorption correction was done using SADABS, and an initial model in space group *Pbcm* was derived by the intrinsic phasing method using SHELXT (Sheldrick 2015b). SHELXL-2016 (Sheldrick 2015a) was used for the refinement of the structure. Difference Fourier syntheses enabled location of H atom positions associated with the single H_2O group, Ow1, which were refined with restraints of 0.84(3) Å on the O–H distances and 1.34(3) Å for H–H distances. No restraints were used for the H atom displacement parameters. Data collection and refinement details are given in Tab. 3, atom coordinates and equivalent isotropic displacement parameters are in Tab. 4, anisotropic displacement parameters are in Tab. 5, selected bond distances are in Tab. 6 and a bond valence analysis is given in Tab. 7.

6.3. Description of the crystal structure

The two symmetrically independent U^{6+} atoms in navrotskyite are coordinated by two multiply bonded apical 'yl' oxygen atoms (O_{yl}) forming the approximately linear uranyl cation $(UO_2)^{2+}$. The uranyl cations are coordinated five-fold equatorially by oxygen atoms of five different SO_4 groups, creating square bipyramids with O_{yl} atoms at the opposing apical vertices of the polyhedron (Burns 2005; Lussier et al. 2016). The U1 polyhedron shares corners with two S2, two S3 and one S4 tetrahedron, while U2 shares corners with two S1, one S2, one S3 and one S5 tetrahedron. The S1, S2 and S3 tetrahedra link adjacent U1 and U2 polyhedra into infinite chains that extend

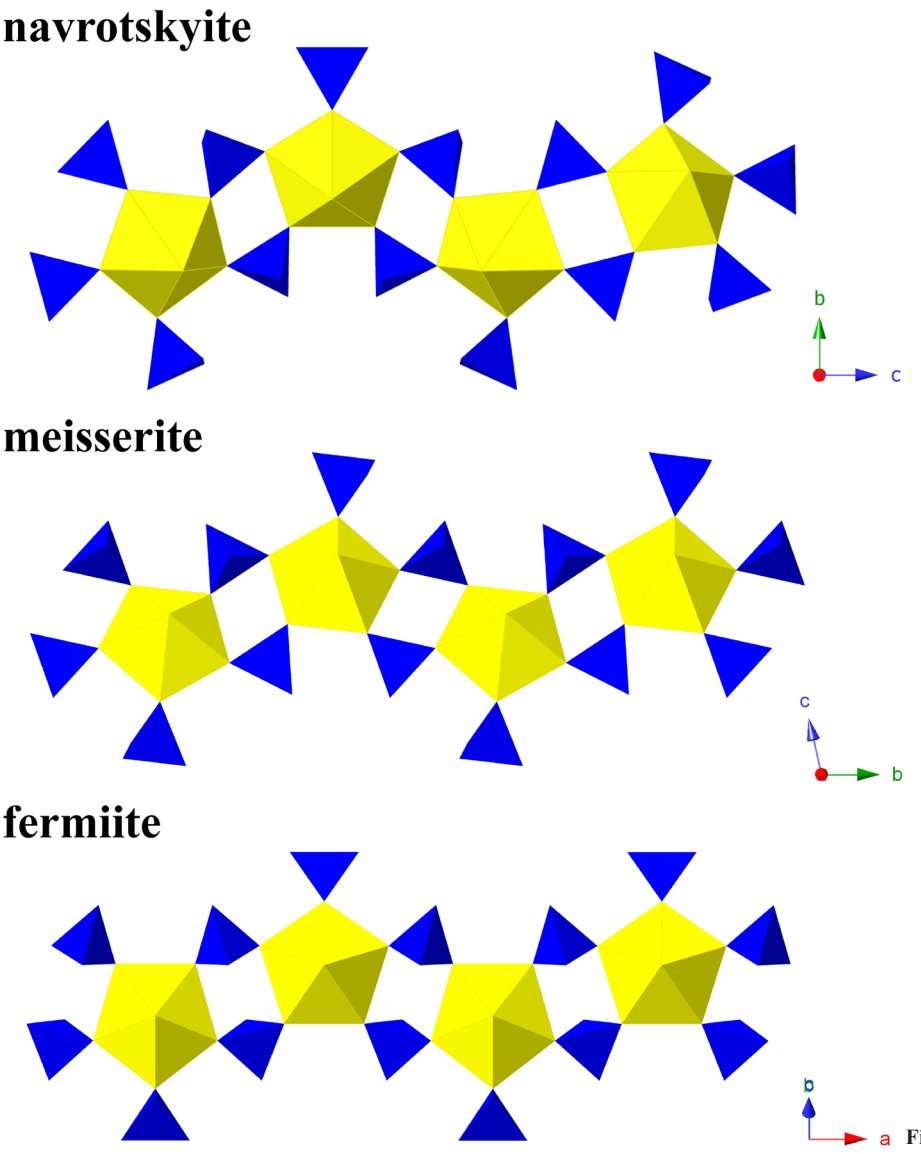

Fig. 4 A comparison of the chain topologies in navrotskyite, meisserite and fermiite.

along [100], producing a $[(UO_2)(SO_4)_3]^{4-}$ structural unit. The chains are also decorated by S4 and S5 tetrahedra that link next-neighbor chains *via* a complex network of K-O and Na-O polyhedra (Fig. 3).

The seven unique Na atom positions in navrotskyite each exhibit irregular coordination geometries and form between five to eight bonds with oxygen atoms of SO_4 groups and O_{yl} atoms, serving to link together multiple $[(UO_2)(SO_4)_3]^{4-}$ chains. Atoms Na1, Na2 and Na5 each have variable coordination numbers between six and eight and bond to oxygen atoms of SO_4 groups and to one O_{yl} atom each. Atoms Na3, Na4 and Na6 are seven or eight-coordinated and bond solely with oxygen atoms of SO_4 groups. Na7 forms a five-coordinated distorted square pyramid with half occupancy that links two chains together through the S1 and S5 tetrahedra attached to U2. The single unique K position is nine-coordinated and forms a dimeric arrangement with itself and binds together multiple chains through SO_4 tetrahedra (2 × S3, 2 × S4, S5) and O21, the O_{yl} atom of U1. The single H_2O group (Ow1, H1A, H1B) forms strong hydrogen bonds with oxygen atoms of two nearby SO_4 groups, O2 (Ow1–H1A···O2; 2.87 Å) and O19 (Ow1–H1B···O19; 2.91 Å) (Tab. 5).

Identical topologies based on the UL_3-type chain (Lussier et al. 2016) are also observed in the minerals fermiite, $Na_4(UO_2)(SO_4)_3(H_2O)_3$ (Kampf et al. 2015) and meisserite, $Na_5(UO_2)(SO_4)_3(SO_3OH)(H_2O)$ (Plášil et al. 2013), and a related topology is found in pseudomeisserite-(NH_4), $(NH_4)_2Na_4[(UO_2)_2(SO_4)_5](H_2O)_4$ (Kampf et al. 2020), all of which occur in the same general assemblage as navrotskyite (Fig. 4). Pseudomeisserite-(NH_4) contains a related UL_3 chain fragment that constitutes part of a more complex uranyl sulfate band. The chain

Tab. 6 Selected bond distances (Å) for navrotskyite.

U1−O6	2.401(4)	Na2−O5	2.409(5)	Na7−O2	2.717(13)
U1−O6	2.401(4)	Na2−O5	2.409(5)	Na7−O18	2.494(16)
U1−O12	2.369(4)	Na2−O6	2.846(5)	Na7−O18	2.439(17)
U1−O12	2.369(4)	Na2−O6	2.846(5)	Na7−Ow1	2.269(14)
U1−O15	2.381(6)	Na2−O8	2.339(5)	Na7−Ow1	2.320(13)
U1−O20	1.756(7)	Na2−O8	2.339(5)	<Na7−O>	2.448
U1−O21	1.761(6)	Na2−O20	2.309(7)		
<U1−O_{Ur}>	1.759	<Na2−O>	2.397	S1−O1	1.459(5)
<U1−O_{Eq}>	2.384			S1−O2	1.463(5)
		Na3−O2	2.348(5)	S1−O3	1.494(5)
U2−O3	2.541(4)	Na3−O9	2.931(7)	S1−O4	1.491(4)
U2−O4	2.399(4)	Na3−O10	2.397(5)	<S1−O>	1.477
U2−O7	2.320(4)	Na3−O16	2.399(5)		
U2−O11	2.342(4)	Na3−O17	2.349(5)	S2−O5	1.457(5)
U2−O19	2.361(4)	Na3−O18	2.746(5)	S2−O6	1.488(5)
U2−O22	1.766(4)	Na3−O18	2.746(5)	S2−O7	1.471(5)
U2−O23	1.770(4)	Na3−Ow1	2.413(6)	S2−O8	1.471(5)
<U2−O_{Ur}>	1.768	<Na3−O>	2.541	<S2−O>	1.472
<U2−O_{Eq}>	2.393				
		Na4−O5	2.674(5)	S3−O9	1.437(6)
K1−O9	2.892(6)	Na4−O5	2.674(5)	S3−O10	1.458(5)
K1−O10	2.709(5)	Na4−O8	2.391(5)	S3−O11	1.482(5)
K1−O12	3.125(6)	Na4−O8	2.391(5)	S3−O12	1.466(5)
K1−O13	2.933(5)	Na4−O13	2.298(7)	<S3−O>	1.461
K1−O14	2.780(5)	Na4−O14	2.497(6)		
K1−O15	3.104(4)	Na4−O14	2.497(6)	S4−O13	1.457(7)
K1−O16	3.053(5)	<Na4−O>	2.489	S4−O14	1.466(5)
K1−O17	3.071(5)			S4−O14	1.466(5)
K1−O21	2.939(4)	Na5−O5	2.480(5)	S4−O15	1.499(7)
<K1−O>	2.956	Na5−O8	2.364(5)	<S4−O>	1.472
		Na5−O14	2.449(5)		
Na1−O1	2.424(5)	Na5−O16	2.317(5)	S5−O26	1.454(5)
Na1−O1	2.424(5)	Na5−O17	2.363(5)	S5−O45	1.457(5)
Na1−O3	2.668(5)	Na5−O22	2.665(5)	S5−O93	1.474(5)
Na1−O3	2.668(5)	<Na5−O>	2.440	S5−O61	1.500(5)
Na1−O4	2.627(4)			<S5−O>	1.471
Na1−O4	2.627(4)	Na6−O1	2.439(5)		
Na1−O23	2.597(5)	Na6−O2	2.816(6)		
Na1−O23	2.597(5)	Na6−O3	2.584(5)		
<Na1−O>	2.579	Na6−O9	2.232(7)		
		Na6−O10	2.332(6)		
		Na6−O18	2.646(6)		
		Na6−O23	3.086(6)		
		<Na6−O>	2.591		

Hydrogen bonds

D–H··*A*	*D*–H	H··*A*	*D*··*A*	<*DHA*
Ow1-H1A··O2	0.84(2)	2.06(3)	2.87(1)	163(7)
Ow1-H1B··O19	0.82(2)	2.25(4)	2.91(1)	137(5)

topologies in each phase differ in the relative orientation of SO_4 tetrahedra and adjoining U-S-U polyhedra exhibit torsion from planarity in the order (in degrees), pseudomeisserite-(NH_4) (85.3/9.2) > navrotskyite (65.8/20.1/2.1) > meisserite (51.9/9.2) > fermiite (7.1/5.6). The torsion angle examined here is defined between adjacent U atoms and the two connecting oxygen atoms of SO_4 groups (U-O-O-U); with two such arrangements forming one link of the chain (Fig. 4). This trend may be a response to increasing cation content or cationic size, whereby bulky K^+ and NH_4^+ cations induce the highest distortions in the pseudomeisserite-(NH_4) and navrotskyite chains.

Acknowledgements. We thank Dr. Nicolas Meisser for his helpful comments that improved the manuscript. A portion of this study was funded by the John Jago Trelawney Endowment to the Mineral Sciences Department of the Natural History Museum of Los Angeles County.

Tab. 7 Bond valence analysis for navrotskyite. Values are expressed in valence units.*

	U1	U2	K1	Na1	Na2	Na3	Na4	Na5	Na6	Na7	S1	S2	S3	S4	S5	H	Σ_{anion}
O1				0.18 ×2 ↓					0.17		1.55						1.90
O2						0.21			0.07	0.15 ×2 ↓	1.54					0.16	2.05
O3		0.35		0.10 ×2 ↓					0.12		1.42						1.99
O4		0.47		0.11 ×2 ↓							1.43						2.01
O5					0.18 ×2 ↓		0.10 ×2 ↓	0.15				1.56					1.99
O6	0.47 ×2 ↓				0.06 ×2							1.44					1.98
O7		0.56										1.50					2.06
O8					0.22 ×2 ↓		0.19 ×2 ↓	0.20				1.50					2.11
O9			0.12			0.05			0.28				1.64				2.09
O10			0.19			0.19			0.22				1.55				2.15
O11		0.53											1.46				2.00
O12	0.51 × 2 ↓		0.07										1.52				2.10
O13			0.11				0.24							1.52			1.98
O14			0.16				0.15 ×2 ↓	0.17						1.52			2.00
O15	0.49		0.07 ×2 →											1.40			2.04
O16			0.08			0.19		0.23							1.57		2.06
O17			0.08			0.21		0.20							1.56		2.05
O18						0.08 ×2 ↓→			0.10	0.16 ×2 ↓					1.49		1.92
O19		0.51													1.40	0.15	2.06
O20	1.85				0.23												2.08
O21	1.83		0.11 ×2 →														2.04
O22		1.81						0.10									1.91
O23		1.79		0.12 ×2					0.04								1.95
Ow1						0.18				0.24 ×2 ↓						–0.15, –0.16	0.11
Σ_{cat}	6.12	6.03	0.98	1.00	1.16	1.19	1.11	1.05	1.00	1.10	5.94	6.01	6.18	5.97	6.02		

*All cation–O bond valence parameters are from Gagné and Hawthorne (2015). Hydrogen-bond strengths are based on O–O bond lengths from Ferraris and Ivaldi (1988).

References

Bartlett JR, Cooney RP (1989) On the determination of uranium–oxygen bond lengths in dioxouranium(VI) compounds by Raman spectroscopy. J Mol Struct 193: 295–300

Burns PC (2005) U^{6+} minerals and inorganic compounds: Insights into an expanded structural hierarchy of crystal structures. Canad Mineral 43: 1839–1894

Chenoweth WL (1993) The Geology and Production History of the Uranium Deposits in the White Canyon Mining District, San Juan County, Utah. Utah Geological Survey Miscellaneous Publications 93–3: pp 1–26

Ferraris G, Ivaldi G (1988) Bond valence vs bond length in O…O hydrogen bonds. Acta Crystallogr B44, 341–344

Gagné OC, Hawthorne FC (2015) Comprehensive derivation of bond-valence parameters for ion pairs involving oxygen Acta Crystallogr B71: 562–578

Gurzhiy VV, Plášil J (2019) Structural complexity of natural uranyl sulfates Acta Crystallogr B75: 39–48

Kampf AR, Plášil J, Kasatkin AV, Marty J, Čejka J (2015) Fermiite, $Na_4(UO_2)(SO_4)_3 \cdot 3H_2O$, and oppenheimerite, $Na_2(UO_2)(SO_4)_2 \cdot 3H_2O$, two new uranyl sulfate minerals from the Blue Lizard mine, San Juan County, Utah, USA. Mineral Mag 79: 1123–1142

Kampf AR, Olds TA, Plášil J, Nash BP, Marty J (2020) Pseudomeisserite-(NH4), a new mineral with a novel uranyl-sulfate linkage from the Blue Lizard mine, San Juan County, Utah, USA. Mineral Mag 84: 1–27

Kampf AR, Olds TA, Plášil J, Marty J, Perry SN, Corcoran L, Burns PC (2021) Seaborgite, $LiNa_6K_2(UO_2)(SO_4)_5(SO_3OH)(H_2O)$, the first uranyl mineral containing lithium Amer Miner 106: 105–111

Lussier AJ, Burns PC, King-Lopez R (2016) A revised and expanded structure hierarchy of natural and synthetic hexavalent uranium compounds Canad Mineral 54: 177–283

Mandarino JA, Glad THB, Dale S (1976) The Gladstone-Dale relationship – Part l: Derivation of new constants Canad Mineral 14: 498–502

Plášil J, Buixaderas E, Cejka J, Sejkora J, Jehlicka J, Novak M (2010) Raman spectroscopic study of the uranyl sulphate mineral zippeite: low wavenumber and U-O stretching regions. Anal Bioanal Chem 397: 2703–2715

Plášil J, Kampf AR, Kasatkin AV, Marty J, Škoda R, Silva S, Čejka J (2013) Meisserite, $Na_5(UO_2)(SO_4)_3(SO_3OH)(H_2O)$, a new uranyl sulfate mineral from the Blue Lizard mine, San Juan County, Utah, USA. Mineral Mag 77: 2975–2988

Pouchou JL, Pichoir F (1985) "PAP" (ϕρZ) procedure for improved quantitative microanalysis. In: Armstrong JT (ed) Microbeam Analysis, San Francisco Press pp 104–106

Sheldrick GM (2015a) Crystal structure refinement with *SHELXL*. Acta Crystallogr C71: 3–8

Sheldrick GM (2015b) *SHELXT* – Integrated space-group and crystal-structure determination. Acta Crystallogr A71: 3–8

Warr LN (2021) IMA-CNMNC approved mineral symbols Mineral Mag 85: 291–320